

Convergence Rate of Model Reference Adaptive Control with Application to Building HVAC Systems

Tumin Wu

*Department of EECS
University of Tennessee
Knoxville, TN, USA
twu19@vols.utk.edu*

Mohammed M. Olama

*Computational Sciences and Engineering Division
Oak Ridge National Laboratory
Oak Ridge, TN, USA
olamahassem@ornl.gov*

Seddik M. Djouadi

*Department of EECS
University of Tennessee
Knoxville, TN, USA
mdjouadi@utk.edu*

Abstract—Model reference adaptive control (MRAC) has been studied for decades and successfully applied in multiple areas, including heating, ventilation, and air conditioning (HVAC) systems for buildings. MRAC is efficient in capturing the time-varying characteristics of buildings' indoor temperatures and outdoor weather environments. In this paper, the rate of convergence of MRAC is investigated, where a direct adaptive control with temperature set point reference tracking is used to regulate the indoor temperatures for buildings. Numerical results show that by controlling the HVAC systems of residential buildings using MRAC, the indoor temperatures converge Q-sublinearly to the desired temperature set points. In addition, the rate of convergence for MRAC is compared with a baseline adaptive model-free control method.

I. INTRODUCTION

Due to the high demand of electricity in the United States for the industrial, commercial, and residential buildings' consumption, there has recently been a grown interest in improving the energy efficiency of buildings [1]. Heating, ventilation, and air conditioning (HVAC) systems are the most electricity/energy consumption units in buildings [2], hence tremendous work has been devoted towards improving their energy efficiency, in addition to improving their energy flexibility in order to support ancillary grid services.

Adaptive control methods [3] [4] have been widely used for controlling HVAC systems, as they address the time-varying behaviors of buildings' dynamics together with the existing uncertainties. Various adaptive control methodologies have been established over the years, and the Model Reference Adaptive Control (MRAC) strategy is considered as one of its main branches. MRAC has widely been used in many other industrial applications, such as in flight control [5] [6] and cruise control for vehicles [7].

This manuscript has been authored by UT-Battelle, LLC under Contract No. DE-AC05-00OR22725 with the U.S. Department of Energy. The United States Government retains and the publisher, by accepting the article for publication, acknowledges that the United States Government retains a non-exclusive, paid-up, irrevocable, world-wide license to publish or reproduce the published form of this manuscript, or allow others to do so, for United States Government purposes. The Department of Energy will provide public access to these results of federally sponsored research in accordance with the DOE Public Access Plan (<http://energy.gov/downloads/doe-public-access-plan>).

MRAC aims at updating the parameters of the control law in order to allow the corresponding closed-loop system behavior to become as close as possible to a given reference model. In particular, model-based adaptive control [2], [8], [9], [10] and model predictive control [1], [11] strategies have been introduced, where both control strategies require accurate physical models that define the system dynamics, which are hard to obtain in practice. Model-free adaptive control strategies [12], [13] are data-driven strategies that control dynamical (building HVAC) systems to maintain their responses (indoor temperatures) as close as possible to the desired reference signals (temperature set points).

The MRAC strategy is efficient in capturing the time-varying characteristics of buildings' indoor temperatures and outdoor weather environments. Examining its convergence helps us better understand how fast/slow it adapts to the time-varying dynamic changes in the environments, such as the changes in weather conditions (outdoor temperature and solar radiation) and the changes of buildings' indoor heat gains and thermal activities. Fast convergence is preferable for fast cooling/heating of building to improve occupants satisfaction. In this paper, we investigate the speed of convergence of a direct MRAC strategy, which maintains the room temperatures of buildings as close as possible to the desired temperature set points. Analytical formulation for the rate of convergence of MRAC is derived. Numerical results show that the indoor temperature for a residential building converges with order one to the desired temperature set point. In addition, a comparison is conducted between the proposed MRAC strategy and the well-known adaptive model-free control (MFC) strategy in [12].

This paper is organized as follows. Section II provides a brief background about three topics addressed in this paper. It initially introduces the thermal model of a residential building HVAC system that is used to generate the simulated indoor temperature data in this study. Then, the adaptive MFC strategy in [12] is introduced, which is used as a baseline control strategy for comparison. Finally, the mathematical definitions of the order and rate of convergence for a sequence are

provided. In section III, we introduce the MRAC strategy and investigate its rate of convergence. Section IV presents a numerical case study that illustrates the rate of convergence of the MRAC strategy and compares it with the baseline adaptive MFC strategy. Finally, the conclusion is presented in Section V.

II. REVIEW OF BUILDING THERMAL MODEL, ADAPTIVE MODEL-FREE CONTROL, AND RATE OF CONVERGENCE

A. Residential Building HVAC Thermal Model

The residential building HVAC thermal model is represented by the widely-used typical one-dimensional thermal resistance-capacitance (RC) model in [14], [15], in which the indoor temperature is governed as follows:

$$\dot{T} = \frac{1}{RC_1}T_{out} - \frac{1}{RC_1}T + \frac{1}{C_1}Q_{out} + \frac{COP}{C_1}Q_{HVAC} \quad (1)$$

where T , T_{out} , and Q_{out} are, respectively, the indoor air temperature, outdoor air temperature, and solar irradiance; R and C_1 are, respectively, the thermal resistance and capacitance of the building; Q_{HVAC} is the cooling power of the HVAC unit; and COP is the coefficient of performance of the HVAC unit. We denote the state vector $x = [T]$, the input of HVAC unit $u = [Q_{HVAC}]$, and the disturbances $w = [T_{out}, Q_{out}]$. Then, we write the state-space form of the residential building thermal model as:

$$\begin{aligned} \dot{x} &= Ax + Bu + Gw \\ y &= Cx + Du \end{aligned} \quad (2)$$

where the system matrices are parameterized as:

$$\begin{aligned} A &= \frac{-1}{RC_1}, & B &= \frac{-COP}{C_1}, \\ G &= \begin{bmatrix} \frac{1}{RC_1} & \frac{1}{C_1} \end{bmatrix}, & C &= 1, D = 0, \end{aligned} \quad (3)$$

and $R = 1/200$, $C_1 = 20a_d v_a c_p$, $COP = 4.5$. Here $a_d = 1.225 \text{ kg/m}^3$ is the air density, $v_a = 550 \text{ m}^3$ is the volume of the air, and $c_p = 1033 \text{ J/kgC}$ is the specific heat of air. The continuous time HVAC thermal model in (2)-(3) is used in this study as a discrete-time model with a 10-minute discretization time step.

B. Model-free Control

The MFC strategy is adopted in this study as a baseline for comparison. It was initially introduced in [16] and then adapted for building load control and demand response in [12]. The single-input single-output (SISO) HVAC system model in (2) is approximated by an ultra-local model as [16]:

$$\dot{y} = F + \alpha u \quad (4)$$

where u and y are the input (power input) and output (indoor temperature) of the (building HVAC) system, F describes the known/unknown system dynamics and is continuously

updated, α is a non-physical scaling parameter such that αu and \dot{y} have the same magnitude. For the estimation, F is approximated by a piece-wise constant function \tilde{F} given as [16]:

$$\tilde{F} = \frac{-6}{L^3} \int_{t-L}^L [(L - 2\sigma)y(\sigma) + \alpha\sigma(L - \alpha)u(\sigma)]d\sigma \quad (5)$$

Here, \tilde{F} is estimated using the previous L measurements of the system. Using the updated F , the "intelligent" proportional control law is expressed as [16]:

$$u = -\frac{\tilde{F} - \dot{y}^* + K_p(y - y^*)}{\alpha} \quad (6)$$

where y^* is the desired reference trajectory (indoor temperature set point) and K_p is the proportional control gain. By combining (4) and (6), we obtain the following error dynamics [16]:

$$\dot{e} + K_p e = 0 \quad (7)$$

Here, $e = y - y^*$ is the tracking error. The value of K_p is obtained from the solution of the differential equation (7) and updated at every time step. Hence, the tuning of the MFC controller is straightforward, since only the parameters α and L are required to be set. A sufficiently small value is needed for the parameter L , and α can be determined from collected input-output measurements as $\alpha = \dot{y}/u$. For more details on the adopted MFC strategy, we refer the reader to [12].

C. Rate of Convergence

The order of convergence and rate of convergence represent how quickly a convergent sequence approaches its limit. A sequence T_k that converges to T^* is said to have order of convergence $q > 1$ and rate of convergence μ if [17]:

$$\lim_{k \rightarrow \infty} \frac{|T_{k+1} - T^*|}{|T_k - T^*|^q} = \mu \quad (8)$$

And the sequence is said to converge Q-sublinearly to T^* (i.e. slower than linearly) if:

$$\lim_{k \rightarrow \infty} \frac{|T_{k+1} - T^*|}{|T_k - T^*|} = 1 \quad (9)$$

A practical method to calculate the order of convergence for a sequence is to calculate the following sequence, which converges to q [18]:

$$q \approx \frac{\log \left| \frac{T_{k+1} - T_k}{T_k - T_{k-1}} \right|}{\log \left| \frac{T_k - T_{k-1}}{T_{k-1} - T_{k-2}} \right|} \quad (10)$$

In the next section, the MRAC strategy is introduced together with the HVAC system model.

III. MODEL REFERENCE ADAPTIVE CONTROL STRATEGY

Initially, we assume that the buildings' parameters are known and constants, then an appropriate distributed strategy is proposed to achieve the control objectives. This process is helpful in order to find the appropriate structure for the adaptive control strategy. In this study, we investigate the convergence rate for a single building HVAC system. The temperature tracking error is defined as $e = T - T_{ref}$, which needs to be minimized for the HVAC unit, where T_{ref} is the temperature set point. The tracking error dynamics are derived from (1) and defined as follows:

$$\dot{e} = -\frac{1}{RC_1}e - \frac{COP}{C_1}u + \frac{1}{RC_1}T_{out} - \frac{1}{RC_1}T_{ref} \quad (11)$$

The discretized version of the temperature error dynamics in (11) using a sampling period of T_s is described by

$$e(k+1) = \alpha_d e(k) + b_d [u(k) + \frac{1}{RC_1}T_{out}(k) - \frac{1}{R \times COP}T_{ref}(k)] \quad (12)$$

where $e(k)$ is the value of $e(t)$ at time $t = kT_s$ and $\alpha = \frac{1}{RC_1}$, $\alpha_d = e^{-\alpha T_s}$, $b_d = \frac{\frac{1}{RC_1}(1 - e^{-\alpha T_s})(-COP)}{C_1}$, $T_s = 600$ seconds (10 minutes). The control strategy is designed based on the discrete error dynamics (12), where the structure of each local control input $u_i(k)$ is given by [8], [9]:

$$u(k) = -K_e e(k) - K_1 T_{out}(k) + K_2 T_{ref}(k) \quad (13)$$

where K_e, K_1, K_2 are the control gains and can be computed as:

$$K_e = \frac{\alpha_m - \alpha_d}{b_d}, K_1 = \frac{1}{R \times COP}, K_2 = \frac{1}{COP} \quad (14)$$

and α_m is a design parameter that determines the speed of temperature change, which is set to be 0.5 in this study. In reality, however, there will be many uncertainties which may impact the system parameters. This leads us to consider a more realistic model where the system parameters are time varying. An adaptive control strategy should be able to track the parameters' variations and achieve the desired performance. The control input of the local controller for the HVAC units can thus be generalized to [8]:

$$u_i(k) = -K_e(k)e(k) - K_1(k)T_{out}(k) + K_2(k)T_{ref}(k) \quad (15)$$

where (15) is based on the structure of the constant-gain control input (13). The adaptive law to estimate the gains K_e, K_1, K_2 directly enables the system to achieve the temperature target when the system parameters change over time. In other words, the gains K_e, K_1, K_2 are chosen such that the controller cancels the effect of disturbances (outside temperature and solar irradiance in our study) and ensures the closed-loop stability of the system. In order to compute these gains, we re-write the temperature error equation (12) in the form of the following linear parametric model [8] [10]:

$$z(k) = \Theta(k)^T \Phi(k) \quad (16)$$

where

$$z(k) = e(k) - \alpha_m e(k-1) \\ \Theta(k) = [b_d K_e(k) \quad b_d K_1(k) \quad b_d K_2(k)]^T \quad (17)$$

$$= [\theta_1(k) \quad \theta_2(k) \quad \theta_3(k)]^T$$

$$\Phi(k) = [u(k-1), T_{out}(k-1), T_m(k-1)] \quad (18)$$

Then, the estimated control gains can be extracted as follows [10]:

$$K_e(k) = \frac{\theta_1(k)}{b_d}, K_1(k) = \frac{\theta_2(k)}{b_d}, K_2(k) = \frac{\theta_3(k)}{b_d} \quad (19)$$

where

$$\Theta(k) = [\theta_1(k), \theta_2(k), \theta_3(k)]^T \\ = \Theta(k-1) + \sqrt{a(k)}P(k)\Phi(k)\epsilon(k) \\ \epsilon(k) = \frac{e(k) - \alpha_m e(k-1)}{m^2(k)} \\ \hat{P}(k) = \frac{1}{\beta(k)} [P(k-1) \\ - \frac{a(k)P(k-1)\Phi(k)\Phi^T(k)P(k-1)}{m^2(k) + a(k)\Phi^T(k)P(k-1)\Phi(k)}] \\ m(k) = 1 + T_s \Phi^T P(k-1)\Phi(k) \\ a \in (0, 1) \\ \beta \in (0, 1) \quad (20)$$

and $P_i(0) = P_0 = P_0^T > 0$. We apply the discrete modified least square (LS) algorithm to compute the estimated gains (more details can be found in [3] [4]). Here, $a_i(k)$ and $\beta_i(k)$ are the weighting factor and the forgetting factor, respectively. $a_i(k)$ is used in the weighted least squares algorithm, while $\beta_i(k)$ allows to give more weight (importance) to the most recent measurements in the estimation algorithm. Both $a_i(k)$ and $\beta_i(k)$ are positive numbers and also can be chosen as constants.

Since the error equation (12) is a linear time varying system, its solution in terms of the state transition matrix is given as:

$$e(k) = \Psi(k, 1)e(1) + \sum_{\tau=1}^{k-1} \Psi(k, \tau+1)B(\tau)g(\tau) \quad (21)$$

where Ψ is the following state transition matrix

$$\Psi(k, k_0) = \begin{cases} I, & \text{if } k = k_0 \\ \prod_{n=k_0}^k A'(n) & \text{if } k > k_0 \end{cases} \quad (22)$$

$A'(n) := \alpha_d - b_d K_e(n)$ is the system matrix,

$$B(\tau) := \left[\frac{1}{R \times COP} - \frac{\theta_2(\tau)}{\theta_1(\tau)} \quad \frac{\theta_3(\tau)}{\theta_1(\tau)} - \frac{1}{R \times COP} \right] \quad (23)$$

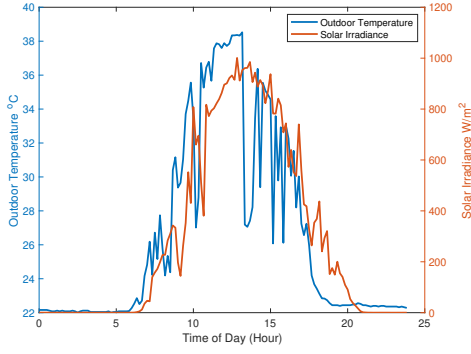


Fig. 1. A sample pair of outdoor temperature and solar irradiance profiles.

and

$$g(\tau) := [T_{out}(\tau) \quad T_m(\tau)] \quad (24)$$

IV. SIMULATION RESULTS

A. Weather and Solar Irradiance Profiles

The outdoor temperature and solar irradiance weather profiles were collected from the typical meteorological year 3 (TMY3) weather data of Las Vegas, NV [19]. Only outdoor temperature and solar irradiance profiles in a summer season are considered. Fig. 1 shows a sample pair of outdoor temperature and solar irradiance profiles for a typical summer day which are fed as the system disturbances. Next, simulation results will be presented and discussed.

B. Results of MRAC

In this section, numerical results for applying MRAC on residential HVAC system are presented. The performance of MRAC is compared with the baseline MFC approach introduced in Section II-B. Fig. 2 shows that using MRAC the indoor temperature tracks a sinusoidal reference temperature set point very well. Only small tracking error is observed in the peaks and valleys of the sinusoidal reference signal. Note that there is no external disturbance applied while generating the results in Fig. 2. Next, we fix the temperature set point at 23°C and apply the external disturbances (outdoor temperature and solar irradiance profiles in Fig. 1) to the residential building model. In this case, Fig. 3 shows the tracking error for MRAC using both the discrete-time temperature error equation in (12) and its solution in terms of the state transition matrix in (21). It is observed that using MRAC the indoor temperature converges to the temperature set point, but it is sensitive to the external disturbances in the middle of the day, especially to the outdoor temperature. It is also observed that the results generated using (12) and (21) coincide with each other; this validates the correct analytical derivation of (21), which is further used in determining the speed of convergence of the MRAC.

Fig. 4 compares the performance of MRAC with that of MFC. It is observed that the indoor temperature using MRAC converges faster than MFC to the temperature set point. However, as observed, MFC is less sensitive to external disturbances at the middle of the day than that of MRAC. Fig. 5 shows the rate of convergence for both MRAC and MFC. We observe that $\mu_{MRAC} > \mu_{MFC}$ at the beginning of the day, after that μ_{MRAC} converges to almost 1, which means the indoor temperature converges Q-sublinearly (i.e. slower than linearly) to the temperature set point 23°C . Fig. 6 shows the order of convergence for MRAC. It is observed that it is less than 1 most of the time; this explains the sensitivity to the large external disturbances at the middle of the day.

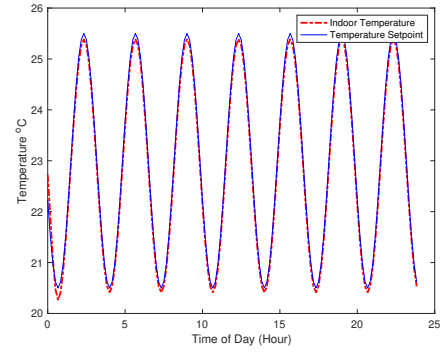


Fig. 2. Indoor temperature tracking performance using MRAC without external disturbances.

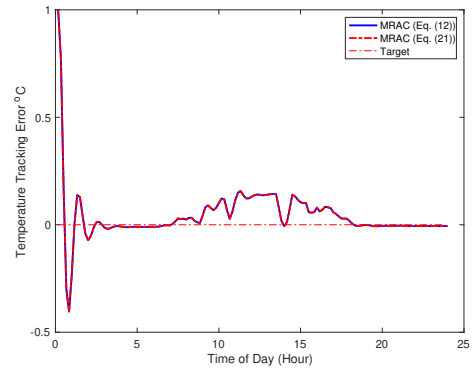


Fig. 3. Tracking error for MRAC with external disturbances.

V. CONCLUSION

In this paper, we investigated the speed of convergence for MRAC while taking into consideration the time-varying characteristics of thermal buildings' behaviors. The rate of convergence for MRAC was compared with that of MFC. Numerical results showed that the convergence rate for MRAC was higher than that of MFC, however, it was more sensitive to external disturbances. In addition, MRAC required more

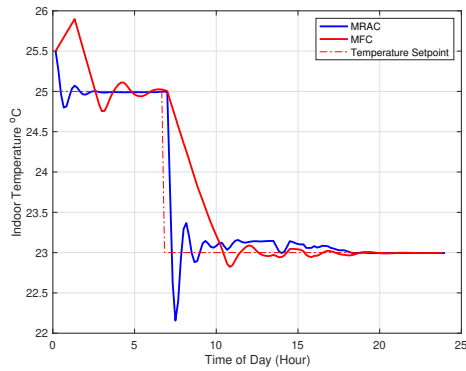


Fig. 4. Indoor temperature comparison between MRAC and MFC.

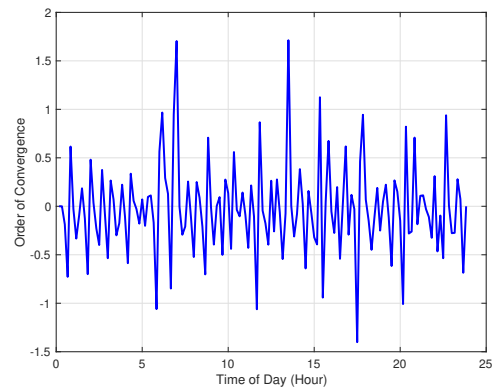


Fig. 6. Order of convergence for MRAC.

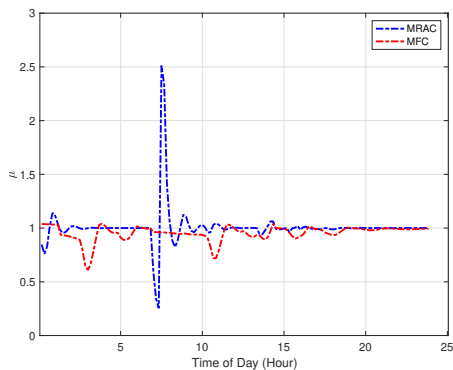


Fig. 5. Rate of convergence of MRAC and MFC.

computational cost than MFC. Future work is to investigate the performance of MRAC in real buildings.

ACKNOWLEDGEMENT

This material is based upon work supported by the U.S. Department of Energy, Office of Energy Efficiency and Renewable Energy, Building Technologies Office under contract DE-AC05-00OR22725.

REFERENCES

- [1] J. Dong, M. Olama, T. Kuruganti, J. Nutaro, C. Winstead, Y. Xue, and A. Melin, "Model predictive control of building on/off hvac systems to compensate fluctuations in solar power generation," in *2018 9th IEEE International Symposium on Power Electronics for Distributed Generation Systems (PEDG)*, pp. 1–5, IEEE, 2018.
- [2] W. Tumin, M. M. Olama, and S. M. Djouadi, "Adaptive control for residential hvac systems to support grid services," in *2021 IEEE Power & Energy Society Innovative Smart Grid Technologies Conference (ISGT)*, pp. 01–05, IEEE, 2021.
- [3] P. Ioannou and B. Fidan, *Adaptive control tutorial*. SIAM, 2006.
- [4] P. A. Ioannou and J. Sun, *Robust adaptive control*. Courier Corporation, 2012.
- [5] Z. Zhao, G. Cruz, and D. S. Bernstein, "Adaptive spacecraft attitude control using single-gimbal control moment gyroscopes without singularity avoidance," *Journal of Guidance, Control, and Dynamics*, vol. 42, no. 11, pp. 2342–2355, 2019.

- [6] Z. Zhao, G. Cruz, T. Lee, and D. S. Bernstein, "Adaptive attitude control of a dual-rigid-body spacecraft with unmodeled nonminimum-phase dynamics," in *2018 Annual American Control Conference (ACC)*, pp. 2503–2508, IEEE, 2018.
- [7] V. Milanés, S. E. Shladover, J. Spring, C. Nowakowski, H. Kawazoe, and M. Nakamura, "Cooperative adaptive cruise control in real traffic situations," *IEEE Transactions on intelligent transportation systems*, vol. 15, no. 1, pp. 296–305, 2013.
- [8] G. Lymeropoulos and P. Ioannou, "Distributed adaptive hvac control for multi-zone buildings," in *2019 IEEE 58th Conference on Decision and Control (CDC)*, pp. 8142–8147, IEEE, 2019.
- [9] G. Lymeropoulos and P. Ioannou, "Building temperature regulation in a multi-zone hvac system using distributed adaptive control," *Energy and Buildings*, vol. 215, p. 109825, 2020.
- [10] G. Lymeropoulos, P. M. Papadopoulos, P. Ioannou, and M. M. Polycarpou, "Distributed adaptive control of air handling units for interconnected building zones," in *2020 American Control Conference (ACC)*, pp. 4207–4212, IEEE, 2020.
- [11] T. Wu, M. M. Olama, S. M. Djouadi, J. Dong, Y. Xue, and T. Kuruganti, "Signal temporal logic control for residential hvac systems to accommodate high solar pv penetration," in *2020 IEEE Power & Energy Society Innovative Smart Grid Technologies Conference (ISGT)*, pp. 1–5, IEEE, 2020.
- [12] B. Telsang, S. Djouadi, M. Olama, T. Kuruganti, J. Dong, and Y. Xue, "Model-free control of building hvac systems to accommodate solar photovoltaic energy," in *2018 9th IEEE International Symposium on Power Electronics for Distributed Generation Systems (PEDG)*, pp. 1–7, IEEE, 2018.
- [13] B. Telsang, M. Olama, S. Djouadi, J. Dong, and T. Kuruganti, "Stability analysis of model-free control under constrained inputs for control of building hvac systems," in *2019 American Control Conference (ACC)*, pp. 5878–5883, IEEE, 2019.
- [14] S. Karaman, R. G. Sanfelice, and E. Frazzoli, "Optimal control of mixed logical dynamical systems with linear temporal logic specifications," in *2008 47th IEEE Conference on Decision and Control*, pp. 2117–2122, IEEE, 2008.
- [15] D. S. Callaway, "Tapping the energy storage potential in electric loads to deliver load following and regulation, with application to wind energy," *Energy Conversion and Management*, vol. 50, no. 5, pp. 1389–1400, 2009.
- [16] M. Fliess and C. Join, "Model-free control," *International Journal of Control*, vol. 86, no. 12, pp. 2228–2252, 2013.
- [17] B. Bockelman, "Rates of convergence," tech. rep., University of Nebraska-Lincoln (United States), 2005.
- [18] J. R. Senning, "Computing and estimating the rate of convergence," tech. rep., Gordon College (United States), 2019.
- [19] M. Sengupta, Y. Xie, A. Lopez, A. Habte, G. Maclaurin, and J. Shelby, "The national solar radiation data base (nsrdb)," *Renewable and Sustainable Energy Reviews*, vol. 89, pp. 51–60, 2018.